An electrochemical method to rapidly assess the environmental risk of silver release from nanowire transparent conductive films

Brenda Omaña-Sanz, Djadidi Toybou, Ludovic Lesven, Valérie Gaucher, Alexandre Fadel, Ahmed Addad, Philippe Recourt, Delphine Yeghicheyan, Devrah Arndt, Caroline Celle, et al.

An electrochemical method to rapidly assess the environmental risk of silver release from nanowire transparent conductive films

Brenda Omaña-Sanz[a*], Djadidi Toybou[b,c], Ludovic Lesven[d], Valerie Gaucher[e], Alexandre Fadel[e], Ahmed Addad[e], Philippe Recourt[a], Delphine Yeghicheyan[f], Devrah Arndt[g], Caroline Celle[c], Jean-Pierre Simonato[c], Christopher Vulpe[g], Laurent Charlet[b], Sophie Sobanska[h], Benjamin Gilbert[i], Annette Hofmann[a*]

[a] Univ. Lille, CNRS, Univ. Littoral Côte d'Opale, UMR 8187, LOG, Laboratoire d'Océanologie et de Géosciences, F 59000 Lille, France
[b] Institut des Sciences de la Terre, Université de Grenoble–Alpes, CNRS, F-38000 Grenoble Cedex 9, France;
[c] Laboratoire d'Innovation pour les Technologies des Energies Nouvelles et les Nanomatériaux, Département des Technologies des Nouveaux Matériaux, Université de Grenoble–Alpes, Commissariat à l'Énergie Atomique et aux Énergies Alternatives, F-38054 Grenoble Cedex 9, France;
[d] Lasir CNRS UMR 8516, University of Lille, 59 655 Villeneuve d'Ascq Cedex, France ;
[e] Univ. Lille, CNRS, INRA, ENSCL, UMR 8207 - UMET - Unité Matériaux et Transformations, F-59000 Lille, France;
[f] Service d'Analyse des Roches et des Minéraux (SARM) CRPG, CNRS UMR 7358, Université de Lorraine, BP20, 54501 Vandoeuvre-lès-Nancy, France
[g] University of Florida Center for Environmental and Human Toxicology, 2187 Mowry Road, Gainesville, Florida, 32611, USA
[h] Institut des Sciences Moléculaires, UMR CNRS 5255, Université de Bordeaux, 33405 Talence, France;
[i] Energy Geoscience Division, Lawrence Berkeley National Laboratory, Berkeley, CA 94720

Keywords

Silver nanowire networks – polysiloxane coatings – electrochemical corrosion – accelerated aging – silver exposure

ABSTRACT

Silver nanowires (AgNW) are new nanomaterials designed to be incorporated into transparent conductive films in electronics, microelectrodes, heated surfaces and others. Although in these films, the AgNW are generally protected by a coating material, a risk for release of silver at all stages of the nanoproduct life cycle does exist due to corrodibility of the metal. Since ionic and nanoparticulate Ag represent a toxicological risk for a large number of living cells, there is a need for quantifying the potential Ag release from these product components. We developed an electrochemical method to evaluate possible corrosion activity of silver in AgNW transparent conductive films (TCFs) and concomitant Ag^+ release. A polysiloxane polymer was used as protective coating of AgNW TCFs. A consistent correlation is observed between the degree of corrosion and the coatings' characteristics, in particular the thicknesses. A major advantage of the new approach, compared to classical aging studies, is the short experimentation time: 20 min are sufficient for a diagnostic result. The method is an accelerated corrosion and release test. It is green methodology with use of very low electric power and with no harmful reagents. A particularly attractive application could be in the field of environmental risk assessment of metals from portable electronics and biosensors.

*Corresponding authors.

E-mail addresses: annette.hofmann@univ-lille.fr (A. Hofmann), brenda.omana-sanz@univ-lille.fr (B. Omaña-Sanz).

1. Introduction

Silver nanowires (AgNWs) are one of the most promising alternative engineered nanomaterials (ENMs) to replace indium tin oxide (ITO) in transparent electrodes (Sannicolo et al., 2016). Random networks of AgNWs are being used for transparent conductive films (TCFs) to be applied in a wide range of technological applications from optoelectronics to heatable films and biomedical devices (Doganay et al., 2016; He and Ye, 2015; Toybou et al., 2019; Zhang and Engholm, 2018). The interconnection of metallic nanowires, e.g. AgNWs, creates electric conductive paths allowing electrical current flow.

It is known that metallic silver is corroded when exposed to atmospheric conditions; similarly silver nanowires are also easily corroded (Graedel, 1992; Molleman and Hiemstra, 2017), thereby causing failures in conductive networks. To counter this problem, application of a nano to micrometer thick layer of a protective coating material over the conductive NW network, before its integration into a device, is often performed in order to stop the diffusion of water vapor and gases, thus to avoid corrosion. Other external damages like scratches and bends are also avoided by this protection.

Different materials have been considered for creation of a protective coating, including reduced graphene oxide (Ahn et al., 2012; Duan et al., 2019), metal oxides and carbonates (Jeong et al., 2019; Khan et al., 2018), optical adhesive (Miller et al., 2013), chitosan (Jin et al., 2017), and polymers (Chen et al., 2014; Kim et al., 2015; Miao et al., 2019; Moreno et al., 2013; Xu and Zhu, 2012). Although the coatings could delay corrosion, 100 % of effectiveness on the long-term still remains an issue (Deignan and Goldthorpe, 2017; Jiu et al., 2015). A noticeable factor is that most of the protective coating materials in use, especially polymers have some degree of permeability at the molecular level.

Besides the permeability aspect, wear and tear of the NW containing products throughout their life cycle, i.e. from their active use to end-of-life disposal, may degrade the mechanical and chemical quality of the conductive film and enhance the corrosion of the nanowires.

Corrosion is responsible for the release of ionic silver and the formation of nanoscopic wire debris. These forms of silver are toxic at low levels to aquatic organisms and microorganisms, and to certain types of human cells (Lehmann et al., 2018; Liao et al., 2019). Corrosion of AgNW TCFs may lead to critical silver exposure of the device user and/or to pollution of the receiving environment.

According to the inventory of available databases e.g. the Nanodatabase, R-Nano and StatNano (R-Nano.fr, https://www.r-nano.fr; STATNANO, https://statnano.com/; The Nanodatabase, http://nanodb.dk/), the number of household products and biomedical devices incorporating nano-silver is rapidly expanding (Bodycap, http://www.bodycap-medical.com/fr/; Naidu et al., 2015; Rajski et al., 2019; Yao et al., 2017). Despite this fact, there is currently a lack of information on toxicological (Lehmann et al., 2019) and eco-toxicological effects of this widespread occurrence of trace silver. Studies concerning silver release have mainly focused on textiles (Part et al., 2018). Standardized risk assessment methods for nanowires is still missing.

Very few predictive models of Ag-ENM fate in the environment have been conducted with data from provenances other than textiles (Giese et al., 2018; Sun et al., 2016). Concerning silver nanowires, previous studies mainly focused on technical quality control of AgNW transparent electrodes, in particular on lifetime stability of the devices (Deignan and Goldthorpe, 2017; Elechiguerra et al., 2005; Jiu et al., 2015; Khaligh and Goldthorpe, 2013; Lin et al., 2018; Mayousse et al., 2015). To our knowledge, this is the first investigation to evaluate the capacity of AgNW in TCFs to corrode (hereafter referred to as corrodibility), in order to assess the risk of metal release to users and the environment. In this work, we developed an electrochemical method where corrosive conditions are imposed on AgNW TCF under aqueous conditions, to evaluate the potential for formation of ionic silver and tiny debris of nanowires and their transport from inside to outside the conducting film. An

accelerated corrosion test is developed, completed within 20 min. Moreover, it can be considered green methodology as only very low electric power is needed and no chemical reagents other than tiny amounts of standard electrolyte salt are used.

The paper reports corrosion experiments conducted with AgNW films, either uncoated or coated with a protective layer of anti-scratch varnish AE12® of different thicknesses. Some AgNW films underwent natural alteration prior to experiments. These samples were considered as "pre-aged" and representative of nanoproducts during their life cycle or at end of life. Two commercial products were also investigated.

2. Materials and Methods

2.1. AgNW film samples

AgNW networks were deposited on large dimension transparent flexible substrate (10 x 10 cm) of polyethylene naphthalate (PEN), called hereafter "AgNW large plate". These large plates were used to prepare the "AgNW film" samples used in the corrosion experiments. The synthesis of AgNWs was conducted following the polyol method, the preparation of the large plates is described in Mayousse et al. (2013). The initial sheet resistances of AgNW large plates varied from 8 to 26 Ω/□. The nanowires used had diameters in the range 50-90 nm and lengths between 6-26 µm (SI appendix, Table S1) according to control measurements conducted with ImageJ software on FESEM images.

The AgNW large plates, when received, had an age of several months to more than one year and thus showed different degrees of aging. A thorough electron microscopic investigation was conducted on each plate before use, in order to discard damaged specimens not suitable for the experiments, or amenable to misleading interpretations.

To prepare the AgNW film samples, the AgNW large plates described above were cut into 2.5 x 3.5 cm^2 pieces, hereafter referred to as AgNW TCF or AgNW film. At least 3 samples

were prepared from each AgNW large plate in order to assure reproducibility of results. Part of the samples were coated with a polysiloxane polymer (anti-scratch varnish AE12®, from ISOCHEM) used as a non-conductive coating material to protect the AgNW films used in the experiments (see details in SI appendix). Coating thicknesses of 500 and 700 nm (mean values) were achieved by varying the spin coating parameters. Polysiloxane is one of the materials studied as potential candidate for TCF coatings. According the findings by Toybou (2018), this coating effectively preserves the AgNW TCF under ambient degradation conditions and seems to improve initial conduction performances of the samples.

In addition, AgNW films of 2.5 x 3.5 cm^2 size, readily coated (by dip coating) with a protective layer of 5µm thickness (mean value), were prepared from new materials that had not undergone any aging prior to the experiments in this study.

Two commercial products were also tested with the method developed here. A silver antibacterial textile (silver-coated fibers) and heatable glasses from a skiing goggle containing silver ENM. Both products were purchased specifically for the experiments. The skiing goggle glasses were composed of a layer containing the ENMs and protected with a very thick over-coating layer of a polymer called polycarbonite by the manufacturer. For the experiments, both materials were cut into pieces of 2.5 x 3.5 cm^2.

2.2. Sample characterization

The effect of the corrosion experiments on the AgNW films were evaluated by Field Emission Scanning Electron Microscopy (FESEM) using a JEOL JSM-7800F LV equipped with EDS/EBSD system, and a FEI Quanta 200 environmental scanning electron microscope (ESEM). The observations by FESEM were performed at 5 kV on coated AgNW films and at 15 kV on uncoated AgNW films. The observations by ESEM were conducted at 20 kV. Both secondary electron (SE) and electron backscattering (BSE) modes of imaging were used. To

158 avoid surface charging, samples were chromium coated (70 Å) by electro-sputting under
159 vacuum prior to FESEM observations.

160 Atomic force microscopy (AFM) topographic observations and roughness measurements
161 were carried out on a Dimension 3100 apparatus from Digital Instruments operated in
162 Tapping Mode, using a set-point amplitude ratio close to 0.9 in order to reduce indentation
163 effects and thereby optimize the topographic contrast. The Nanoworld silicon SPM sensors
164 had a tip radius less than 10 nm, the nominal spring constant and resonance frequency of the
165 cantilever being around respectively 50 N m^{-1} and 250 kHz.

166 *2.3. Corrosion cell*

167 The corrosion experiments were carried out in an electrochemical cell in a three electrode
168 configuration (Figure 1). The AgNW film of 2.5 x 3.5 cm^2 was used as the anode, a platinum
169 grid of similar size as the cathode. A mercury/mercurous sulfate electrode was used as
170 reference. The electrochemical cell, specially designed for the experiments, made of PTFE,
171 consists of a rectangular chamber of 10 mL volume, with two facing walls of the size of the
172 electrodes. In the chamber top, slots are foreseen for positioning cathode and anode, and a
173 hole for insertion of the reference electrode. The inter-electrode distance between anode and
174 cathode is 0.5 cm. The reference electrode (RE-2CP, ALS Co.) is located outside the anode-
175 cathode path. The electrolyte is introduced into the chamber through another small hole in the
176 chamber top. An automatic titrator (Titroline 7000, SI Analytics) controls solution addition.

177 All experiments were performed in a Faraday cage. A potentiostat (VSP, Bio-Logic) served
178 to set the cell potential and to record the current generated.

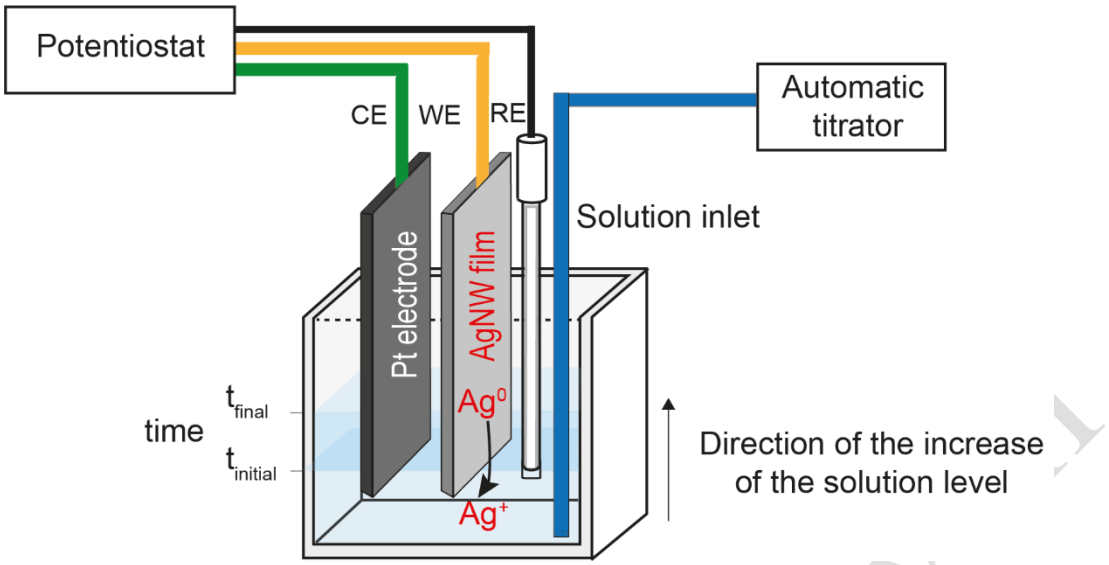

Figure 1. Schematic of the electrochemical corrosion cell used in the corrosion tests. A three-electrode configuration was used: the AgNW film was used as anode (working electrode WE), a platinum grid as cathode (counter electrode CE), a mercury/mercurous sulfate electrode as reference electrode (RE). The automatic titrator allowed constant addition of solution over the duration of the experiment ($t_{final} - t_{initial}$ = 20 min). The arrow shows the direction of increase of the solution level, thus the progression of the provoked corrosion.

2.4. Experimental conditions

$NaNO_3$ at 0.01 M was used as electrolyte solution (SI appendix, Figure S1). This concentration is representative of environmental conditions of continental surface and subsurface waters (Stumm and Morgan, 1996). The 0.01 M $NaNO_3$ salt solution established naturally at a pH of 5.0 ± 0.2. This pH was retained as the working pH because it was well within the range where polysiloxane is chemically stable (SI appendix) and because this pH is representative for environmental conditions.

We determined the free corrosion potential (E_{corr}) of a 2 mm silver rod (Advent Research Materials) and of commercial AgNW (2.23% wt/wt dispersion, Nanogap) dispersed onto a carbon paste electrode. The corrosion potential of these silver materials was 0.45 V, detailed results can be found in Lehmann et al. (2019). To study corrosion on the AgNW film electrodes, we applied an overpotential of 0.8 V vs. SHE. At this voltage, the nanowires were not subject to any Joule heating problem (Khaligh et al., 2017) neither in the aqueous nor in

the aerial part of the electrode. Also the water electrolysis reaction (E°(pH5) = 0.925 V) is negligibly small at a potential of 0.8 V, thus not interfering with the Ag redox reaction or the pH of the solution.

The $NaNO_3$ electrolyte solutions and the K_2SO_4 0.6 M reference electrode solution were prepared with ultrapure water and analytical grade reagents.

2.5. Experimental procedure

The corrosion experiments were conducted in the electrochemical cell under constant addition of electrolyte solution. This allowed to continuously renewing the solution-air contact line on the film surface. The continuous shifting of this "active zone" allowed maintaining high corrosion conditions throughout the experiment. Some tests were also conducted under fixed electrolyte volume conditions (SI appendix, Figure S2 A-B).

An initial volume of around 2 mL of electrolyte solution was placed in the reactor chamber, just enough to allow the solution surface to touch the lower edge of the AgNW film. The electric potential (set to 0.8V vs. SHE) and the automatic titrator were switched on simultaneously, thus insuring constant addition of solution over the duration of the experiment and starting at time $t_{initial}$ (Figure 1). A total volume of 2 mL of electrolyte solution was added at a flow rate of 100 $\mu L.min^{-1}$ (20 min). This flow rate corresponds to a displacement of the solution/air interface inside the reactor chamber of 0.04 cm/min. Preliminary experiments showed that the chosen rate was enough to ensure a constant shift of the interfacial line between solution and air on the AgNW film. Electron microscopic controls showed that the movement is rapid enough to contain the capillary ascent of solution along the nanowires and along the borders of the film. The solution inside the cell was not stirred but the continuous addition of solution induced some degree of turbulent mixing. The pH of the solution, initially at 5, was controlled before and after the experiment. After 20 min, the experiment was

stopped, the electrodes were removed carefully and an aliquot of the electrolyte solution was taken for Ag^+ analysis. The AgNW film sample was removed from the reactor, the area that had been immersed was cut off, carefully rinsed and placed in a desiccator for later surface analysis. The remaining part of the film, which had not been immersed in the electrolyte solution, was used for a subsequent experiment on the same sample.

All the solution samples were filtered through 0.2 µm pore size polycarbonate filters (PCTE Sartorius, Fisher Scientific), and several samples were additionally filtered through 10 kDa (equivalent to 4 nm) ultrafiltration membranes (Ultracel, Amicon 25 mm, Merck) using a stirred ultrafiltration cell system (Amicon, model 8010, 10 mL, Merck) in order to separate Ag nanoparticles from the truly dissolved fraction. All filtrates were acidified with HNO_3 2% trace analysis/ultrapure quality. Analyses of silver concentrations were conducted by Inductively-Coupled Plasma Mass Spectrometry (ICP-MS Agilent 7700x).

3. Results and discussion

In the electrochemical cell (Figure 1), the oxidation of silver metal is promoted by using the AgNW TCF as the anode and applying an electric potential higher than the corrosion potential. The silver metal is oxidized and goes into solution in the form of ionic silver (eq. 1).

Reaction at the anode (WE): $Ag_{(s)} \leftrightarrow Ag^+_{(aq)} + e^-$ (eq. 1)

In this study, we investigated the corrodibility of polysiloxane coated AgNW films with coating thicknesses varying from thin (500 nm), medium (700 nm) to thick coated (5 µm). Uncoated AgNW films were also studied. Each selected film was submitted to the electrochemical corrosion test. The current response to the applied voltage was recorded via the potenstiostat. The raw and qualitative data was then transformed by integrating the traces over the experiment time, to obtain Q the quantity of charge, i.e. a single number representative of a given experiment (calculation details in SI appendix).

3.1. Features of corrosion after experiments

As mentioned above, the AgNW large plates available for the preparation of the samples, i.e. the "AgNW films" were carefully studied by Field Emission Scanning Electron Microscopy (FESEM) before use to discard damaged specimens not suitable for the experiments. On the plates kept for the study, the signatures of natural pre-aging processes or of synthesis related defects were identified (SI appendix, Figures S3, S4) so that the effects of our corrosion experiment could be clearly recognized.

The characteristic signature of nanowire degradation by electrochemical corrosion (our experiments) appears mainly in the active zone, i.e. along a triple junction line between solution, air and the partly immersed sample. The active zone was continuously renewed by a constant addition of electrolyte solution, thereby maintaining high electrical conduction thus continuous corrosion conditions. Electrochemical corrosion signature was fragmentation of the nanowires into an alignment of nanoparticles and/or nanorods. This feature appeared similarly for uncoated (Figure 2 A-D) and thin-coated AgNW films (Figure 2 E-H). Fragmentation creates discontinuities leading to electrical failure. It has been shown previously that the degradation of an AgNW network is dependent on several network characteristics (Elechiguerra et al., 2005; Mayousse et al., 2015). Our results show that in a given sample, nanowires with smaller diameters were corroded preferentially to thicker nanowires or silver nanoparticle clusters (Figure 2D). When investigating the parameters nanowire diameter and sheet resistance, we observed that small diameters and/or low initial sheet resistances produced higher quantity of charge than large diameters and/or high initial resistances (SI appendix, Figure S5). In other words, corrosion is enhanced in networks with thin nanowires and/or high wire densities (i.e. high initial sheet resistances). Similar trends were described in previous studies (Toybou, 2018).

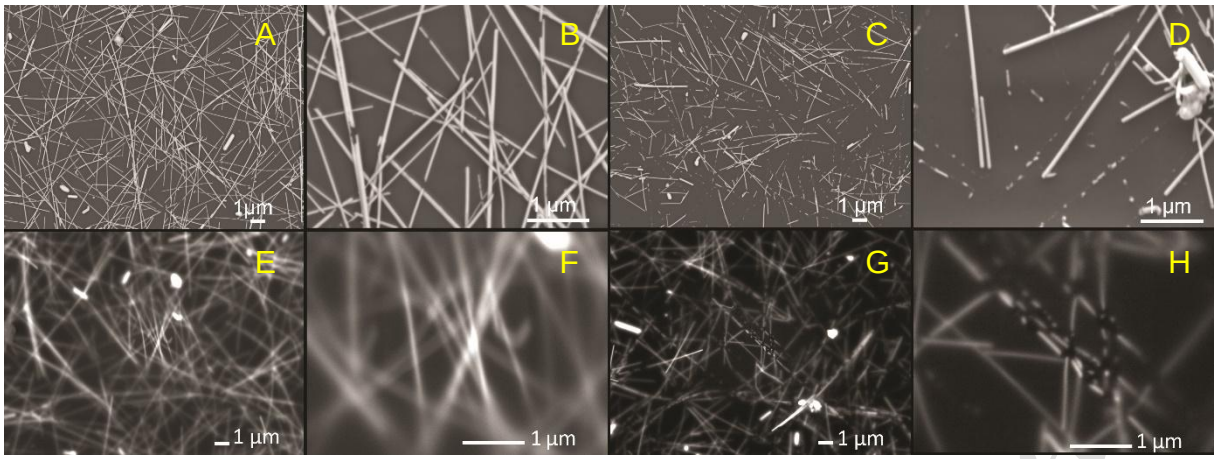

Figure 2. SEM images (BSE) of AgNW films from plate 5 (NW diameter 57 ± 10 nm, NW length 7 ± 2 µm) unexposed and exposed to the corrosion test. Each pair of images (e.g. A-B; C-D, etc) are images of the same film at different magnifications. A-B) Pristine nanowires in an uncoated film, some silver clusters are seen, an evidence that natural corrosion took place prior to experiments. C-D) Fragmentation, nanowire discontinuities and formation of nanoparticles as a result of 20 min of corrosion test. E-F) Pristine nanowires in a film protected with a thin layer of AE12 coating. G-H) Same film after 20 min of corrosion test; fragmented nanowires with dissolution gaps appearing dark. Another example of electrochemical corrosion signatures on AgNW films (from plate 9: NW diameter 86 ± 13 nm nm, NW length ± 4 µm) can be found in SI appendix, Figure S13.

In some spots of the AgNW film, roughening of the nanowire surface was observed together with a decrease in NW brightness. Although this suggested mineral deposition, no evidence of silver oxide, hydroxide or sulfide on the wire surface was detected by EDS (SI appendix, Figure S4) maybe due to low amounts of these products particularly in the case of sulfide, below the detection limits of the technique used (SEM-EDS) as discussed previously by other authors (Lin et al., 2018; Toybou, 2018). It is most probable that the observed roughening was due to overgrowths made essentially of elemental silver (Lin et al., 2018). No sign of melting was observed at NW junctions or at NW tips, discarding the hypothesis of Joule heating (Khaligh et al., 2017) to contribute to wire failure under our experimental conditions.

In AgNW films with medium coating thickness, similar pattern were observed as described above for thin coated and uncoated films, i.e. highly fragmented networks in the active zone and numerous patches of darkened nanowire surfaces (Figure 2 G-H) (Mayousse et al., 2015). Films coated with a thick layer of polymer (5 ± 1µm) could not be investigated by SEM because of insufficiently electron-transparency of that thick layer.

Tiny cubic nanoparticles were observed in some AgNW films (from plates 1 and 9). These nanocubes, precipitates of Ag and Cl, appeared on the surface of nanowires or the surface of the polymer coating in case of coated films. The presence of traces of chlorine in our experimental set-up is attributed to Cl^- impurities contained in AgNW, inherited from the reagents used for NW synthesis and then released upon NW dissolution. Details of this unexpected occurrence of Ag-Cl nanocubes and speciation calculations are discussed in SI appendix, Figures S6-S8.

3.2. Corrosion of AgNWs as a function of coating layer thickness

The presence of a protective layer on AgNW films and the thickness of this layer play a crucial role in limiting corrosion and failure of AgNW films.

Corrosion current responses are presented for four categories of AgNW films (Figure 3.a), from uncoated films to films with a thick coating layer of AE12. Each category includes AgNW films prepared by us (see details in SI appendix Table S1). The results are consistent with expectations, i.e. the developed quantity of charge was higher in experiments with AgNW films with a thin layer of polysiloxane and decreased as the thickness of the protective layer increased (Figure 3.a). For uncoated AgNW films, the quantity of charge developed was lower than for thin coated films, which may reflect loss of NWs during the experiment, due to insufficient adhesion of NWs to the PEN substrate in the unprotected films. It is interesting to highlight that a corrosion current was measured in all cases. Even when the AgNW film was

overcoated with a thick layer (5 µm) of protective AE12, an electrical current could still be measured. Collectively, these results on corrodibility of coated AgNW films indicate that polysiloxane is permeable to water molecules and Ag^{+} ions.

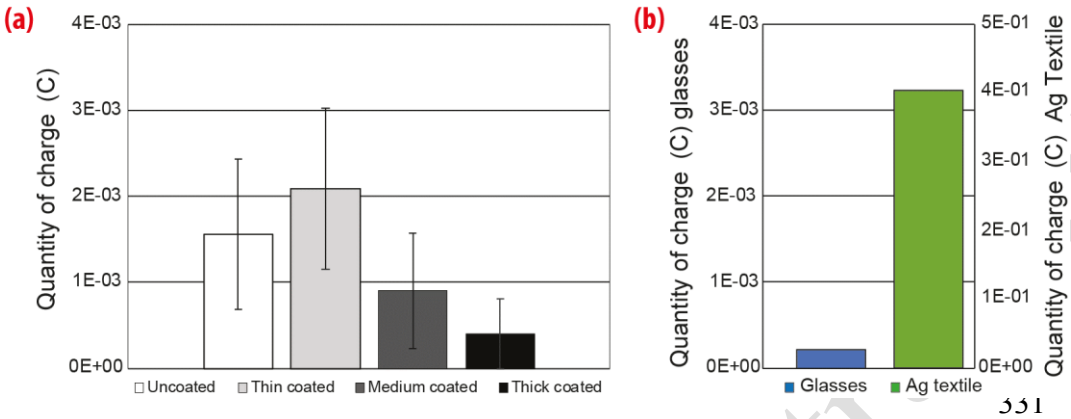

Figure 3. a) Comparison between quantity of charge (mean values) generated in AgNW films with varying thicknesses of polysiloxane coating: uncoated, thin (500 nm), medium (700 nm) and thick (around 5 µm). The high standard deviation values (n= 5) observed in each bar are related to the variable qualities of the different plates used (see SI appendix, Figure S12). b) Quantity of charge for the commercial products tested: heatable glasses containing silver ENM (blue bar) and silver antibacterial textile (green bar). All the results correspond to experiments at 0.01 M ionic strength, imposed potential of 0.8 V vs. SHE and pH 5.

Polymers such as PEDOT:PSS, PVP, PVA, that have often been used as coating materials (Jiu et al., 2015), are hydrophilic polymers with a plurality of polar groups which tend to sorb water. Similarly, AE12 polysiloxane used in the present work is also hydrophilic according to fabricant communication and corroborating results from water contact angle measurements (SI appendix, Figure S9). Celle et al. (2018) reported a water vapor transmission rate of 80 $mg.m^{-2}.d^{-1}$ for a polysiloxane layer of 1.5 µm thickness. The polarity of these polymers confers them some degree of permeability, which explains why ion diffusion is possible through the protective layer, therefore why a corrosion current is measured by the potentiostat.

To control that the coating remained intact throughout the experiment, we conducted AFM surface roughness measurements on the surface of an AgNW thin coated film, on treated and

untreated zones. Results (SI appendix, Figure S10) show no significant difference between roughness values in both zones, indicating that the polymeric material exhibits no textural alteration at a scale of tens of nanometers.

Electrochemical corrosion results of the two commercial products containing silver, a silver antibacterial textile and a skiing goggle with heatable glasses containing silver ENM (Figure 3.b) showed evidence of corrosion in both materials. The skiing goggle glasses (blue bar) generated low corrosion current compared to the quantity of charge measured in the AgNW films of the present study. This result may be related to the very thick layer of protective coating covering the conductive layer. In the case of silver antibacterial textile (green bar), the values were 2 orders of magnitude higher than for the AgNW films.

In the next section, the release of ionic silver during the corrosion test will be investigated quantitatively.

3.3. Quantification of dissolved silver (Ag^+)

Silver released from AgNWs during the corrosion experiments was quantified by ICP-MS. To distinguish between nanoparticulate Ag and truly dissolved Ag^+, the filtration procedure included micro-filtration through a 0.2 µm pore size membrane and ultra-filtration through a 10 kDa membrane. Potential sources of silver contamination as well as interactions between Ag^+ and filter materials (i.e. sorption and desorption) were controlled but proved to be non significant under experimental conditions in this study.

Silver concentration was measured after each filtration step. Total silver was not quantified systematically due to the limitation of sample volume. Results showed no significant difference in concentration between nanoparticulate-dissolved (0.2µm) and truly dissolved (10 kDa) fractions (SI appendix, Figure S11). This strongly suggests that the main transfer path of silver from the AgNW film to the solution was via diffusion of Ag^+ through the

polymer coating, or via direct diffusion in the case of uncoated AgNW film. In consequence, 0.2 um polycarbonate filtrated solutions were considered as true solutions.

In Figure 4.a, concentrations of dissolved silver (originating from AgNW films) are represented as a function of the thickness of the protective coating layer. Clearly, the amount of dissolved silver decreases as the thickness of the protection layer increases. For uncoated films, release of dissolved silver was not significantly higher than for coated films, corroborating the fact that corrosion is limited by detachment of silver nanowires, which thereby modulates the formation of ionic silver. While Figure 4.a shows mean values, single results specific to two given plates are presented in SI appendix, Figure S12.

To find out if a direct relation can be established between the amount of Ag^+ detected in solution (by ICP-MS) and the electrochemical results, we converted the parameters quantity of charge, resulting from the corrosion current measured by the potentiostat, and the amount of ionic silver released from AgNW films to comparable units (calculation details in SI appendix).

As seen in Figure 4.b, the data sets originating from coated films (blue dots) show a same general trend. A linear correlation can be drawn with a slope of almost 1, suggesting that silver corrosion feeds the electric current with almost no electron loss. Although data are somewhat scattered around the correlation line ($R^2 = 0.79$), this result supports the initial hypothesis that the amount of charge determined for an experiment is representative of the amount of silver released to solution. In contrast, the data sets for uncoated films (red dots) result in very scattered data, among which two sets are out of range with an Ag^+/electron ratio close to 2:1. Here the relatively high value for the Ag^+ release may be attributed to loss of nanowire debris to solution, and these debris may have been included in the quantification of silver. Over all the results suggest that the measure of quantity of charge obtained in the

corrosion experiment is a number representative of the amount of corrosion of silver in AgNW films. For coated films, it is directly proportional.

Concerning the quantification of results of the commercial products containing silver, the skiing goggle glasses released small amounts of dissolved silver (40.88 µg/L), comparable to

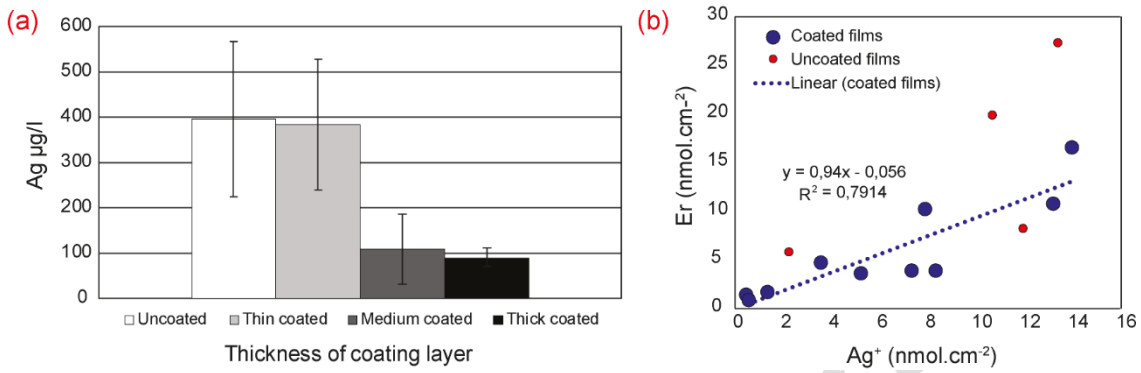

Figure 4. a) Silver concentrations (mean values) in the reactor solutions of the experiments presented in Fig. 3.a. The high standard deviation values (n= 5) are related to the variable qualities of the different plates used (see SI appendix, Figure S12). b) For individual samples, correlation between quantity of electrons released (Er) derived from current measurements by potentiostat and dissolved silver from AgNW films (Ag^+) detected in solution by ICP-MS. Coated films (bleu dots) show good linear relation between both parameters with a slope of almost 1, while uncoated films (red dots) gave rise to more scattered data. Detailed calculations of both parameters in SI appendix.

the levels obtained in the thick coated AgNW films of the present study. Interestingly, indium was also released to solution (7.28 µg/L). EDS analyses suggest the presence of indium oxide in the skiing goggle glasses.

In the case of silver antibacterial textile, the concentration of dissolved silver reached 4.57 $x10^4$ µg/L. The high specific surface area of the silver used as a coating of the textile fibers may explain this very high release.

These first trials on commercial Ag containing household products demonstrate that the corrosion method developed here allows obtaining a rapid estimate on the corrodibility of a silver containing material and on the potential metal release. The application of the method to the antibacterial textile shows that it can be used as well for macro-scale corrodible silver containing compounds.

3.4. Anthropogenic silver release to the environment and potential impacts

When considering all categories of AgNW conductive transparent films investigated in this study, the range of silver concentrations released from the AgNWs films ranged from approximately 90 µg/L to 400 µg/L (0.83 µmol/L to 3.7 µmol/L). These concentrations can be confronted to toxicity data. Ionic silver has been shown to bioaccumulate in various aquatic organisms and to be highly toxic to bacteria, phytoplankton, and aquatic invertebrates and vertebrates with toxicity threshold values typically around 0.2 µg/L (Croteau et al., 2011; Davies, 1978; Farkas et al., 2010; US EPA, https://www.epa.gov/wqc/ambient-water-quality-criteria-silver). These organisms have important roles in the trophic ecosystem as primary producers and consumers, and adverse impacts of silver to these organisms could have detrimental consequences to overall ecosystem health (Glibert, 2012; Vaughn, 2010).

The toxicity of ionic silver to humans depends on the type of cells that are exposed, the liver cells being the most sensitive. According to the American Conference of Governmental Industrial Hygienists (ACGIH, https://www.acgih.org/), the occupational exposure limit for dissolved silver to prevent argyria is 0.01 mg/m^3 (0.01 µg/L).

Overall these limits demonstrate that the silver released during the corrosion test of the AgNW films is orders of magnitude above the levels acceptable for the natural environment and living species, even in the case of a thick protective coating (90 µg/L), thereby they point to the relevancy of this test.

Concerning anthropogenic input of silver to aquatic systems, Zhang et al. (2008) reported concentrations of dissolved silver in the surface water of Tokyo Bay ranging from $6.5x10^{-4}$ µg/L to 1.7 $x10^{-3}$ µg/L, a level also obtained for the surface waters of the Japan Sea. Deycard et al. (2017) found average dissolved concentrations of $1x10^{-3}$ µg/L in river water of the "La Réole site" in France. They also reported that the daily silver concentration in an urban

450 wastewater treatment plant located on the fluvial part of the Gironde estuary, ranged from
451 0.14 to 0.55 µg/L depending on weekday and meteorological conditions.

452 Estimations of nanosilver environmental release are primarily based on modelling
453 approaches. Giese et al. (2018) estimated environmental concentrations of Ag-ENM arising
454 from medical applications to have reached $3.8x10^{-4}$ µg/L in surface fresh waters in Germany
455 in 2017 and predicted an increase to $8.9x10^{-4}$ µg/L for 2030. In sewage treatment effluents,
456 modelling calculations gave $1.89x10^{-2}$ µg/L for 2017 and $3.06x10^{-2}$ µg/L for 2030
457 respectively.

458 Silver released from AgNW films during the corrosion test may be put into the perspective
459 of current background levels of Ag in anthropogenically influenced waters. Indeed the 5-10
460 mL of solution in the electrochemical cell would have to be diluted by an average factor of
461 2000 before "disappearing" in the general background. The diversification of (nano)silver
462 containing products and the increase in their production will irrevocably increase the Ag
463 background concentrations in natural systems and affect water quality.

464 The human body may come in direct contact with silver from anthropogenic source.
465 Deycard et al. (2017) reported that Ag concentrations in a typical household personal care
466 product (deodorant) labeled as containing Ag, range from 0.2 to 0.4 mg/kg of solution (200
467 µg/L to 400 µg/L). These concentrations are within the interval of values generated during our
468 corrosion test. The comparison is appealing because AgNW TCF are predestined to be in
469 contact with skin. Thus, silver released from AgNW TCF may be significant compared to
470 current silver levels in contact with the body.

471

472 *3.5. Relevance of the developed corrosion test*

473 The experimental results obtained in this work on silver corrosion in AgNW films allow us
474 to estimate an average silver corrosion rate of about 3.7×10^{-10} g/s (Calculation details in SI

475 appendix, Table S3), which is a factor 30 larger than the rate measured for the natural
476 dissolution of a noble silver foil in water saturated with air (Graedel, 1992). This comparison
477 highlights the strength of the method developed here, where a corrosion potential, slightly
478 enhanced compared to natural conditions, leads to a fast and easily measurable response of the
479 investigated sample. This method is therefore well adapted to assess the risk of metal release
480 from everyday consumer products to their immediate environment (skin, corporal fluids,
481 effluent waters, aquatic systems).

482 The potential application fields of the accelerated release test are wide, however the field of
483 biosensors appears as a very promising one because the use of wearable electronic sensors
484 containing metallic and in particular nanowire silver is growing and because in these devices,
485 the film electrodes are often located in humid environment and in direct contact with the skin.
486 Moreover biocompatible capping agents e.g. citrate are often used in antibacterial Ag-ENMs,
487 which can enhance silver solubility (Liao et al., 2019).

488 An important aspect also is that the method can be applied at any time in the life cycle of
489 the AgNW film. Nowack and Mitrano (2018) discuss the importance of performing aging-
490 release tests in ENM-nanoproducts during use rather than in pristine materials, as consumers
491 and the environment are mostly exposed to aged and transformed nanomaterials (Baun et al.,
492 2017). The method may play a role in predicting the silver flux from household products,
493 biosensor products and personal electronics containing nano-silver (Steinhäuser and Sayre,
494 2017) during life-time and at end of life. In the case these products come in contact with the
495 environmental water compartment, the method will again provide valuable data for flux
496 estimates.

497 While experiments presented in this work on AgNW coated films have been conducted with
498 a polysiloxane coating (anti-scratch varnish AE12®), more research needs be perform with
499 AgNW films with other matrices, other coatings, in particular hydrophobic polymers like

epoxy or new materials such as optical adhesive or reduced graphene oxide layers, is necessary to work out the method limitations. Reference AgNW TCF materials would also need to be developed with known toxicological characteristics.

The current lack of standard methods to quantify the risk of exposure of ENM enabled devices to the environment, underline the importance of developing the accelerated corrosion method into a standard method for quantifying the releasability of metals from conductive thin films. The way forward will be to constitute a data base for reference conductive films to which new materials could be compared.

4. Conclusions

In this work, we developed an electrochemical method to evaluate the potential corrosion activity of silver in nanowire transparent conductive films (AgNW TCFs), with or without coating (polysiloxane varnish AE12 ®), and the possible release of ionic silver. We have demonstrated that there is a consistent link between the corrosion current response obtained from coated AgNW TCFs, Ag^+ release and the coatings' characteristics. The corrosion current in each experiment is transformed into quantity of charge, a single number representative of the corrodibility of a material. This corrosion indicator is established quickly, 20 minutes are sufficient for a diagnostic result. The method is thus seen as an accelerated corrosion test, with speed being a significant advantage compared to classical aging studies. Additionally, this method is free from harmful reagents and is low power consumption.

Previous works mainly focused on technical quality control of AgNW transparent electrodes, in particular on lifetime stability of the devices. To our knowledge, this is the first investigation of the corrodibility of a conductive nanomaterial under aqueous conditions, in order to assess the risk of metal release to users and the environment.

A significant result obtained with the accelerated corrosion test is the fact that protective coatings of AgNW films do not systematically provide full protection against corrosion of silver and the release of ionic silver to outside the material. Our results demonstrated that even a thick 5 µm layer of protective polysiloxane coating could not stop AgNW corrosion completely, still leaving a risk of silver (Ag^+) release.

The accelerated corrosion method is promising because it tests the degree of isolation of a material by the possibility of electron flow The measure of corrodibility depends not only on the presence of (nano) silver but also on textural parameters, in particular the degree of dispersion of the particles in the material and the characteristics of protective coatings. We suggest that the accelerated corrosion method could be elevated to the level of a standard material quality control method to quantify the risk of silver release by corrosion from (nano)silver containing products.

The method is not strictly limited to the study of AgNW TCFs, and can be adapted to products containing other oxidisable conductive nano-materials, in particular those with oxidation potential below that of water. Several technology-critical elements (TCE), increasingly applied as ENMs, with application fields where toxicology limits are even less well explored, could be targeted.

Abbreviations

AgNW: silver nanowires

Argyria: is a condition caused by excessive exposure to chemical compounds of the element silver, or to silver dust.

ENMs: enginered nanomaterials

ITO: indium tin oxide

Nanoproduct: product containing nanomaterial

PEDOT:PSS : poly(3,4-Ethylenedioxythiophene):poly(StyreneSulfonate)

PEN: polyethylene naphtalate

PTFE: polytetrafluoroethylene

PVA: polyvinyl alcohol

PVP: poly-vinylpyrrolidone

SHE: standard hydrogen electrode

TCF: transparent conductive film

Acknowledgements

This study was conducted in the framework of the project NanoWIR2ES (Nanowire Intelligent Re-Design and Recycling for Environmental Safety) supported by the European Union ERANET-SIINN program (European Research Area Network Safe Implementation of Innovative Nanoscience and Nanotechnology) and was funded by the « Region Hauts de France ». Many thanks to Guillaume Bai (University of Lille) who conducted water contact angle measurements on polysiloxane resin, and Sandra Ventalon (University of Lille) for her help in the spectroscopic observations. We greatly appreciated working with Christophe Vermander (Ecole Centrale de Lille) who realized the electrochemical reactor and Jean Claude Bruyere who helped elucidating the chemical properties of polysiloxane AE12.

Appendix A. Supplementary data

Supplementary data contain complementary information regarding method and results: table of large plates used for preparation of AgNW films, description of coating material and sample preparation, effect of ionic strength on current generation, details on calculation of quantity of charge, experiment results under fixed electrolyte volume, images showing NW displacement on uncoated films, images highlighting characteristic features of natural

alteration (artifacts) on NW films, effects of NW-network density and NW diameter on current, description of silver-chloride nanocubes and EDS spectra, table of stability constants for silver species, model calculations for aqueous silver speciation, water contact angle measurement on control samples, AFM roughness measurements on coated AgNW films, dissolved silver after micro and ultrafiltration, comparison between unaltered and altered large plates, conversion of Ag+ concentrations and electric current generated to a common unit (nmol.cm^{-2}), details for calculations of corrosion rates, supplementary images illustrating corrosion signatures on AgNWs after corrosion test.

References

Ahn, Y., Jeong, Y., Lee, Y., 2012. Improved Thermal Oxidation Stability of Solution-Processable Silver Nanowire Transparent Electrode by Reduced Graphene Oxide. ACS Applied Materials & Interfaces 4, 6410–6414. https://doi.org/10.1021/am301913w

Baker, D.R., Lundgren, C.A., 2017. Electrochemical determination of the gallium-nitride photocorrosion potential in acidic media. J. Mater. Chem. A 5, 20978–20984. https://doi.org/10.1039/C7TA04545J

Baun, A., Sayre, P., Steinhäuser, K.G., Rose, J., 2017. Regulatory relevant and reliable methods and data for determining the environmental fate of manufactured nanomaterials. NanoImpact 8, 1–10. https://doi.org/10.1016/j.impact.2017.06.004

Bodycap, le compagnon santé connectée. URL http://www.bodycap-medical.com/fr/ (accessed 7.19.19).

Celle, C., Cabos, A., Fontecave, T., Laguitton, B., Benayad, A., Guettaz, L., Pélissier, N., Nguyen, V.H., Bellet, D., Muñoz-Rojas, D., Simonato, J.-P., 2018. Oxidation of copper nanowire based transparent electrodes in ambient conditions and their stabilization by encapsulation: application to transparent film heaters. Nanotechnology 29, 085701. https://doi.org/10.1088/1361-6528/aaa48e

Chen, S., Song, L., Tao, Z., Shao, X., Huang, Y., Cui, Q., Guo, X., 2014. Neutral-pH PEDOT:PSS as over-coating layer for stable silver nanowire flexible transparent conductive films. Organic Electronics 15, 3654–3659. https://doi.org/10.1016/j.orgel.2014.09.047

Croteau, M.-N., Misra, S.K., Luoma, S.N., Valsami-Jones, E., 2011. Silver Bioaccumulation Dynamics in a Freshwater Invertebrate after Aqueous and Dietary Exposures to Nanosized and Ionic Ag. Environmental Science & Technology 45, 6600–6607. https://doi.org/10.1021/es200880c

Davies, P., 1978. Toxicity of silver to rainbow trout (Salmo gairdneri). Water Research 12, 113–117. https://doi.org/10.1016/0043-1354(78)90014-3

Deignan, G., Goldthorpe, I.A., 2017. The dependence of silver nanowire stability on network composition and processing parameters. RSC Advances 7, 35590–35597. https://doi.org/10.1039/C7RA06524H

Deycard, V.N., Schäfer, J., Petit, J.C.J., Coynel, A., Lanceleur, L., Dutruch, L., Bossy, C., Ventura, A., Blanc, G., 2017. Inputs, dynamics and potential impacts of silver (Ag) from urban wastewater to a highly turbid estuary (SW France). Chemosphere 167, 501–511. https://doi.org/10.1016/j.chemosphere.2016.09.154

Doganay, D., Coskun, S., Genlik, S.P., Unalan, H.E., 2016. Silver nanowire decorated heatable textiles. Nanotechnology 27, 435201. https://doi.org/10.1088/0957-4484/27/43/435201

Duan, F., Li, W., Wang, G., Weng, C., Jin, H., Zhang, H., Zhang, Z., 2019. Can insulating graphene oxide contribute the enhanced conductivity and durability of silver nanowire coating? Nano Research 12, 1571–1577. https://doi.org/10.1007/s12274-019-2394-8

Elechiguerra, J.L., Larios-Lopez, L., Liu, C., Garcia-Gutierrez, D., Camacho-Bragado, A., Yacaman, M.J., 2005. Corrosion at the Nanoscale: The Case of Silver Nanowires and Nanoparticles. Chemistry of Materials 17, 6042–6052. https://doi.org/10.1021/cm051532n

Farkas, J., Christian, P., Urrea, J.A.G., Roos, N., Hassellöv, M., Tollefsen, K.E., Thomas, K.V., 2010. Effects of silver and gold nanoparticles on rainbow trout (Oncorhynchus mykiss) hepatocytes. Aquatic Toxicology 96, 44–52. https://doi.org/10.1016/j.aquatox.2009.09.016

Giese, B., Klaessig, F., Park, B., Kaegi, R., Steinfeldt, M., Wigger, H., von Gleich, A., Gottschalk, F., 2018. Risks, Release and Concentrations of Engineered Nanomaterial in the Environment. Scientific Reports 8. https://doi.org/10.1038/s41598-018-19275-4

Glibert, P.M., 2012. Ecological stoichiometry and its implications for aquatic ecosystem sustainability. Current Opinion in Environmental Sustainability 4, 272–277. https://doi.org/10.1016/j.cosust.2012.05.009

Graedel, T.E., 1992. Corrosion mechanisms for silver exposed to the atmosphere. Journal of the Electrochemical Society 139, 1963–1970.

He, W., Ye, C., 2015. Flexible Transparent Conductive Films on the Basis of Ag Nanowires: Design and Applications: A Review. Journal of Materials Science & Technology, A Special Issue on 1D NanomaterialsSynthesis, Properties, and Applications 31, 581–588. https://doi.org/10.1016/j.jmst.2014.11.020

Jeong, Y.-C., Nam, J., Kim, J., Kim, C., Jo, S., 2019. Enhancing Thermal Oxidation Stability of Silver Nanowire Transparent Electrodes by Using a Cesium Carbonate-Incorporated Overcoating Layer. Materials 12, 1140. https://doi.org/10.3390/ma12071140

Jin, Y., Wang, K., Cheng, Y., Pei, Q., Xu, Y., Xiao, F., 2017. Removable Large-Area Ultrasmooth Silver Nanowire Transparent Composite Electrode. ACS Applied Materials & Interfaces 9, 4733–4741. https://doi.org/10.1021/acsami.6b15025

Jiu, J., Wang, J., Sugahara, T., Nagao, S., Nogi, M., Koga, H., Suganuma, K., Hara, M., Nakazawa, E., Uchida, H., 2015. The effect of light and humidity on the stability of silver nanowire transparent electrodes. RSC Advances 5, 27657–27664. https://doi.org/10.1039/C5RA02722E

Khaligh, H.H., Goldthorpe, I.A., 2013. Failure of silver nanowire transparent electrodes under current flow. Nanoscale research letters 8, 1–6.

Khaligh, H.H., Xu, L., Khosropour, A., Madeira, A., Romano, M., Pradére, C., Tréguer-Delapierre, M., Servant, L., Pope, M.A., Goldthorpe, I.A., 2017. The Joule heating problem in silver nanowire transparent electrodes. Nanotechnology 28, 425703.

Khan, A., Nguyen, V.H., Muñoz-Rojas, D., Aghazadehchors, S., Jiménez, C., Nguyen, N.D., Bellet, D., 2018. Stability Enhancement of Silver Nanowire Networks with Conformal ZnO Coatings Deposited by Atmospheric Pressure Spatial Atomic Layer Deposition. ACS Applied Materials & Interfaces 10, 19208–19217. https://doi.org/10.1021/acsami.8b03079

Kim, S., Kim, S.Y., Chung, M.H., Kim, J., Kim, J.H., 2015. A one-step roll-to-roll process of stable AgNW/PEDOT:PSS solution using imidazole as a mild base for highly conductive and transparent films: optimizations and mechanisms. J. Mater. Chem. C 3, 5859–5868. https://doi.org/10.1039/C5TC00801H

Lehmann, S., Gilbert, B., Maffeis, T., Grichine, A., Pignot-Paintrand, I., Clavaguera, S., Rachidi, W., Seve, M., Charlet, L., 2018. In Vitro Dermal Safety Assessment of Silver Nanowires after Acute Exposure: Tissue vs. Cell Models. Nanomaterials 8, 232. https://doi.org/10.3390/nano8040232

Lehmann, S.G., Toybou, D., Pradas del Real, A.-E., Arndt, D., Tagmount, A., Viau, M., Safi, M., Pacureanu, A., Cloetens, P., Bohic, S., Salomé, M., Castillo-Michel, H., Omaña-

Sanz, B., Hofmann, A., Vulpe, C., Simonato, J.-P., Celle, C., Charlet, L., Gilbert, B., 2019. Crumpling of silver nanowires by endolysosomes strongly reduces toxicity. Proceedings of the National Academy of Sciences 201820041. https://doi.org/10.1073/pnas.1820041116

Liao, C., Li, Y., Tjong, S.C., 2019. Bactericidal and Cytotoxic Properties of Silver Nanoparticles. Int J Mol Sci 20. https://doi.org/10.3390/ijms20020449

Lin, C.-C., Lin, D.-X., Jhan, J.-T., 2018. Effects of Environmental Factors on the Stability of Silver Nanowire Transparent Electrodes, in: 2018 IEEE 13th Nanotechnology Materials and Devices Conference (NMDC). Presented at the 2018 IEEE 13th Nanotechnology Materials and Devices Conference (NMDC), IEEE, Portland, OR, pp. 1–4. https://doi.org/10.1109/NMDC.2018.8605897

Mayousse, C., Celle, C., Fraczkiewicz, A., Simonato, J.-P., 2015. Stability of silver nanowire based electrodes under environmental and electrical stresses. Nanoscale 7, 2107–2115. https://doi.org/10.1039/C4NR06783E

Miao, L., Liu, G., McEleney, K., Wang, J., 2019. Epoxy-embedded silver nanowire meshes for transparent flexible electrodes. Journal of Materials Science 54, 10355–10370. https://doi.org/10.1007/s10853-019-03507-7

Miller, M.S., O'Kane, J.C., Niec, A., Carmichael, R.S., Carmichael, T.B., 2013. Silver Nanowire/Optical Adhesive Coatings as Transparent Electrodes for Flexible Electronics. ACS Applied Materials & Interfaces 5, 10165–10172. https://doi.org/10.1021/am402847y

Molleman, B., Hiemstra, T., 2017. Time, pH, and size dependency of silver nanoparticle dissolution: the road to equilibrium. Environmental Science: Nano 4, 1314–1327. https://doi.org/10.1039/C6EN00564K

Moreno, I., Navascues, N., Arruebo, M., Irusta, S., Santamaria, J., 2013. Facile preparation of transparent and conductive polymer films based on silver nanowire/polycarbonate nanocomposites. Nanotechnology 24, 275603. https://doi.org/10.1088/0957-4484/24/27/275603

Naidu, K.S.B., Govender, P., Adam, J.K., 2015. Nano Silver Particles in Biomedical and Clinical Applications : Review 10.

Nowack, B., Mitrano, D.M., 2018. Procedures for the production and use of synthetically aged and product released nanomaterials for further environmental and ecotoxicity testing. NanoImpact 10, 70–80. https://doi.org/10.1016/j.impact.2017.12.001

Part, F., Berge, N., Baran, P., Stringfellow, A., Sun, W., Bartelt-Hunt, S., Mitrano, D., Li, L., Hennebert, P., Quicker, P., Bolyard, S.C., Huber-Humer, M., 2018. A review of the

fate of engineered nanomaterials in municipal solid waste streams. Waste Management 75, 427–449. https://doi.org/10.1016/j.wasman.2018.02.012

Rajski, L., Juda, M., Los, A., Witun, E., Malm, A., 2019. Medical textiles with silver/nanosilver and their potential application for the prevention and control of healthcare-associated infections – mini-review. Current Issues in Pharmacy and Medical Sciences 32, 104–107. https://doi.org/10.2478/cipms-2019-0020

R-Nano.fr. URL https://www.r-nano.fr/ (accessed 7.18.19).

Sannicolo, T., Lagrange, M., Cabos, A., Celle, C., Simonato, J.-P., Bellet, D., 2016. Metallic Nanowire-Based Transparent Electrodes for Next Generation Flexible Devices: a Review. Small 12, 6052–6075. https://doi.org/10.1002/smll.201602581

STATNANO : Nano Science, Technology and Industry Information. URL https://statnano.com/ (accessed 7.18.19).

Steinhäuser, K.G., Sayre, P.G., 2017. Reliability of methods and data for regulatory assessment of nanomaterial risks. NanoImpact 7, 66–74. https://doi.org/10.1016/j.impact.2017.06.001

Stumm, W., Morgan, J.J., 1996. Aquatic Chemistry-chemical equilibria and rates in natural waters. Wiley, 3rd edition.

Sun, T.Y., Bornhöft, N.A., Hungerbühler, K., Nowack, B., 2016. Dynamic Probabilistic Modeling of Environmental Emissions of Engineered Nanomaterials. Environmental Science & Technology 50, 4701–4711. https://doi.org/10.1021/acs.est.5b05828

Toybou, D., 2018. Nanofils d'argent à dimensions maîtrisées: synthèse, toxicité et fabrication d'électrodes transparentes Ph.D. Dissertation, Université de Grenoble-Alpes, FR. 301.

Toybou, D., Celle, C., Aude-Garcia, C., Rabilloud, T., Simonato, J.-P., 2019. A toxicology-informed, safer by design approach for the fabrication of transparent electrodes based on silver nanowires. Environmental Science: Nano. https://doi.org/10.1039/C8EN00890F

US EPA. (1980). Ambient Water Quality Criteria for Silver. URL https://www.epa.gov/sites/production/files/2019-03/documents/ambient-wqc-silver-1980.pdf (accessed 9.27.19).

Vaughn, C.C., 2010. Biodiversity Losses and Ecosystem Function in Freshwaters: Emerging Conclusions and Research Directions. BioScience 60, 25–35. https://doi.org/10.1525/bio.2010.60.1.7

Welcome to The Nanodatabase. URL http://nanodb.dk/ (accessed 7.18.19).

Xu, F., Zhu, Y., 2012. Highly Conductive and Stretchable Silver Nanowire Conductors. Advanced Materials 24, 5117–5122. https://doi.org/10.1002/adma.201201886

Yao, S., Myers, A., Malhotra, A., Lin, F., Bozkurt, A., Muth, J.F., Zhu, Y., 2017. A Wearable Hydration Sensor with Conformal Nanowire Electrodes. Advanced Healthcare Materials 6, 1601159. https://doi.org/10.1002/adhm.201601159

Zhang, R., Engholm, M., 2018. Recent Progress on the Fabrication and Properties of Silver Nanowire-Based Transparent Electrodes. Nanomaterials 8, 628. https://doi.org/10.3390/nano8080628